# Photonic Approach to Multi-band Dual-chirp Microwave Waveform Generation with Quadruple Bandwidth

Haowen Zhang [1, a], Qiuze Yu [1, *]

[1] School of Electronic Information, Wuhan University, Wuhan, 430072, China

[a] yuhenry007@whu.edu.cn

**Abstract.** We propose a scheme for generating a microwave waveform with dual-band, dual-chirp, linearly chirped characteristics and quadruple chirp bandwidth. In this scheme, we employ two cascaded Mach-Zehnder modulators (MZMs), with each modulated by a microwave signal and a linearly frequency modulated (LFM) signal. This modulation technique extends the LFM signal to multiple frequency bands and enhances its bandwidth. By properly adjusting the microwave signal's frequency and the LFM's carrier frequency, we can intelligently combine the up-chirp and down-chirp signals obtained after heterodyne beating in the photodetector (PD). This combination results in the creation of multi-band dual-chirp signals with quadruple chirp bandwidth. Our simulation demonstrates the simultaneous generation of dual-chirp microwave waveforms in the X, Ka, U, and V bands, with central frequency-bandwidth ranges of 10GHz-4GHz, 30GHz-4GHz, 50GHz-4GHz, and 70GHz-4GHz respectively. These dual-chirp signals possess a bandwidth four times that of the driving chirp signal, leading to a Time Bandwidth Product (TBWP) four times greater than that of the driving chirp signal. Consequently, the proposed scheme has the potential to significantly improve range Doppler resolution in modern radar systems. Additionally, the high-frequency and large-bandwidth dual-band dual-chirp LFM signals generated by this approach are anticipated to enhance range resolution and detection range in multitarget radar systems.

**Keywords**: Microwave photonics; DP-DPMZM; Multi-band dual-chirp linearly frequency modulated (LFM) signal; Radar signal.

In modern radar systems, the use of linearly frequency modulated (LFM) signals is prevalent due to their ability to enhance detection range through powerful pulse compression [1]. When high-speed moving objects are detected, radar systems require both high range resolution and velocity resolution, necessitating the emission of a detection signal with a large time-bandwidth product (TBWP) [2]. However, there are limitations to further improving the TBWP and center frequency of the generated LFM signal due to physical device constraints [3]. The utilization of microwave photon technology in LFM signal generation, on the other hand, overcomes these restrictions of electrical equipment, enabling the production of LFM signals with higher center frequencies and larger TBWP [4].

Over the past few years, several microwave photonic methods for generating chirped microwave waveforms have been proposed [5]-[7]. One method [8] applies a direct space-time (DST) mapping approach to generate chirp microwave waveforms with high carrier frequencies; however, this method is bulky and lacks stability. Another method involves spectral shaping with wavelength-to-time mapping (SS-WTT) using dispersion elements to generate chirp microwave waveforms [9]. Nonetheless, the fixed central frequency and temporal duration limitations of a few nanoseconds at most result in a smaller TBWP, thereby reducing radar detection ability. To address these limitations, a scheme for LFM signal generation based on optical external modulation is proposed, effectively improving the time bandwidth product of the chirp signal [10]-[12]. When a radar system emits a single-chirp signal to detect a moving target, the range-Doppler effect introduces a time domain offset, which results in a decrease in ranging accuracy. To address this, dual-chirp microwave waveforms are commonly utilized in radar systems to mitigate the range-Doppler coupling effect and enhance target detection performance [13]. This is achieved by analyzing the arrival time of two chirped microwave waveforms with opposite frequency chirping, effectively canceling out the range-Doppler coupling effect. To overcome the degradation of radar detection performance caused by the range-Doppler coupling effect, a scheme [14] is proposed for

generating dual-chirped signals based on microwave photonics using a dual-parallel Mach-Zehnder modulator (DPMZM).

In complex detection scenarios with multiple targets, single-band radar systems have traditionally faced challenges in achieving accurate results. It has been observed that multi-band radar systems offer additional advantages [15]-[17] compared to their single-band counterparts in various environments. For example, a high-frequency signal in the K-band provides a narrow beam, making it suitable for object tracking, while the signal in the S-band is better equipped to handle adverse weather conditions, making it suitable for warning applications [18]. In recent years, several photonic approaches have been proposed for generating multi-band chirp signals. One such approach, presented in [19], demonstrates a dual-parallel Mach-Zehnder modulator (DPMZM)-based multi-band radar transmitter. This scheme generates a dual-band linear frequency modulated (LFM) signal with quadrupled bandwidth and central frequency, facilitating high range resolution in radar imaging. However, the limited time-bandwidth product (TBWP) of the generated dual-band LFM signal restricts the detection capability of the multi-band radar system. Another approach, described in [20], generates a bandwidth-quadrupled dual-chirp waveform using cascaded Mach-Zehnder modulators (MZMs) without frequency multiplication. The signal is then modulated onto an optical frequency comb (OFC) to generate multi-band LFM signals [21]-[23]. However, the TBWP of the generated multi-band LFM signals is constrained by the baseband driving LFM signal. To increase the temporal duration and bandwidth of the generated multi-band chirp signal, two methods have been proposed: the split parabolic waveform method [24] and the phase-encoded waveform method [25].

In this study, we have implemented a scheme based on the concept proposed in [26] to generate a dual-chirp microwave waveform with an increased number of bands using two cascaded Mach-Zehnder modulators (MZMs). The even-order sidebands are generated through RF modulation using MZM1 and then injected into MZM2, where they are modulated by a single-chirp linear frequency modulated (LFM) signal to introduce a parabolic phase difference between the tones. By carefully adjusting the frequency and amplitude of the RF signal and the carrier frequency of the LFM signal, we are able to generate four-band dual-chirp microwave waveforms with center frequencies that are one, three, five, and seven times the original center frequency, and a quadrupled chirp bandwidth. After undergoing polarization coupling and heterodyne beating in a photodiode (PD), the generated four-band dual-chirp microwave waveform exhibits a high-frequency component, a large bandwidth, and consequently, a large time-bandwidth product (TBWP). Additionally, the autocorrelation analysis of the simulation results reveals a high peak-to-sidelobe ratio (PSR) and excellent pulse compression capabilities. We anticipate that the proposed scheme for generating multi-band dual-chirp LFM signals can be effectively utilized in multi-band radar systems to enhance range resolution and expand the detection range.

## 1. Theory and principle

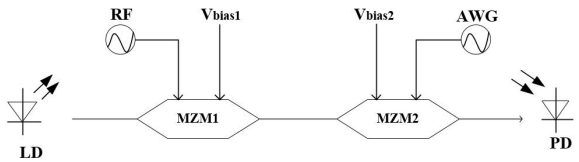

Fig.1 shows the schematic diagram of the multi-band dual-chirp signals generator

with quadruple chirp bandwidth, which consists of a laser diode (LD), two cascaded Mach-Zehnder modulators (MZMs) and a photodiode (PD). The lightwave from the laser diode (LD), expressed as $E_{in}(t)=E_0\exp(j\omega_0 t)$, is injected into MZM1, which is driven by a RF signal $V_1\cos(\omega_1 t)$ and is biased at the minimum transmission point (MITP) to suppress even-order sidebands and optical carrier, and so the output lightwave can be expressed as

$$\begin{aligned} E_{\mathrm{MZM1}}(t) &= \frac{\sqrt{2}}{2}\mathrm{E}_0 \exp(j\omega_c t)\sum_{n=-\infty}^{\infty} J_{2n-1}(\beta_1)\exp\left[j2(n-1)\omega_1 t\right] \\ &\approx J_1(\beta_1)\exp\left[j(\omega_c+\omega_1)t\right]-J_1(\beta_1)\exp\left[j(\omega_c-\omega_1)t\right] \\ &\quad +J_3(\beta_1)\exp\left[j(\omega_c+3\omega_1)t\right]-J_3(\beta_1)\exp\left[j(\omega_c-3\omega_1)t\right] \\ &\quad +J_5(\beta_1)\exp\left[j(\omega_c+5\omega_1)t\right]-J_5(\beta_1)\exp\left[j(\omega_c-5\omega_1)t\right] \end{aligned} \tag{1}$$

where $E_0$ and $\omega_c$ are the amplitude and frequency of the lightwave field from the LD, $\omega_1$ is the frequency of the RF signa, $\beta_1=\pi V_1/V_{\pi 1}$ is the modulation index of MZM1 with a half-wave voltage of $V_{\pi 1}$, and $V_1$ is the amplitude of the RF driving signal. $J_n(\cdot)$ is the n$^{\text{th}}$-order Bessel function of the first kind. The modulation index of MZM1 is adjusted to $\beta_1=3.189$, in order to make the amplitude difference between the up-chirp LFM signals and the down-chirp LFM signals generated after the beating as small as possible. Here the sidebands higher than fifth-order are neglected since they have relative smaller amplitude as the modulation index is not too larger.

Then, the multi-tone lightwaves are modulated by an LFM signal $V_2\cos(\omega_2 t+kt^2)$ via the MZM2 following, which is biased at the maximum point (MATP) in order to suppress the odd-order sidebands. Here $V_2$ and $\omega_2$ are the amplitude and frequency of the LFM signal, respectively, and $k$ is the chirp rate of the input chirped signal, so the lightwaves after the modulation can be written as

$$\begin{aligned} E_{\mathrm{MZM2}}(t) &\approx E_{\mathrm{MZM1}}(t)\cdot\left[1-J_2(\beta_2)\exp j\left(2\omega_2 t+2kt^2\right)+J_2(\beta_2)\exp j\left(-2\omega_2 t-2kt^2\right)\right] \\ &\approx \exp(j\omega_c t)\left\{\begin{bmatrix} J_1(\beta_1)\exp(j\omega_1 t)-J_1(\beta_1)\exp(-j\omega_1 t)+J_3(\beta_1)\exp(j3\omega_1 t) \\ -J_3(\beta_1)\exp(-j3\omega_1 t)+J_5(\beta_1)\exp(j5\omega_1 t)-J_5(\beta_1)\exp(-j5\omega_1 t)\end{bmatrix}\right. \\ &\quad \left.-\begin{Bmatrix} J_1(\beta_1)J_2(\beta_2)\begin{bmatrix}\exp j\left(\omega_1 t+2\omega_2 t+2kt^2\right)-\exp j\left(-\omega_1 t+2\omega_2 t+2kt^2\right) \\ \exp j\left(\omega_1 t-2\omega_2 t-2kt^2\right)-\exp j\left(-\omega_1 t-2\omega_2 t-2kt^2\right)\end{bmatrix} \\ +J_2(\beta_2)J_3(\beta_1)\begin{bmatrix}\exp j\left(3\omega_1 t+2\omega_2 t+2kt^2\right)-\exp j\left(-3\omega_1 t+2\omega_2 t+2kt^2\right) \\ \exp j\left(3\omega_1 t-2\omega_2 t-2kt^2\right)-\exp j\left(-3\omega_1 t-2\omega_2 t-2kt^2\right)\end{bmatrix}\end{Bmatrix}\right\} \end{aligned} \tag{2}$$

where $\beta_2=\pi V_2/2V_{\pi 2}$ is the modulation indices of MZM2 with half-wave voltage of $V_{\pi 2}$.Then, the multi-tone lightwaves are detected by a square-law photodiode pair, and the total output photocurrent is

$$\begin{aligned} I_{PD} &= \eta E_{\mathrm{MZM2}}^{*}(t)\times E_{\mathrm{MZM2}}(t) \\ &\approx \eta\left\{\left[-4J_1(\beta_1)^2 J_2(\beta_2)-4J_2(\beta_2)J_3(\beta_1)^2\right]\cos\left(2\omega_2 t+2kt^2\right)\right. \\ &\quad +\left[2J_1(\beta_1)^2 J_2(\beta_2)-4J_1(\beta_1)J_2(\beta_2)J_3(\beta_1)-2J_2(\beta_2)J_3(\beta_1)J_5(\beta_1)\right]\cos\left(2\omega_1 t-2\omega_2 t-2kt^2\right) \\ &\quad +\left[2J_1(\beta_1)^2 J_2(\beta_2)-4J_1(\beta_1)J_2(\beta_2)J_3(\beta_1)-2J_2(\beta_2)J_3(\beta_1)J_5(\beta_1)\right]\cos\left(2\omega_1 t+2\omega_2 t+2kt^2\right) \\ &\quad +\left[4J_1(\beta_1)J_2(\beta_2)J_3(\beta_1)-2J_1(\beta_1)J_2(\beta_2)J_5(\beta_1)\right]\cos\left(4\omega_1 t-2\omega_2 t-2kt^2\right) \\ &\quad +\left[4J_1(\beta_1)J_2(\beta_2)J_3(\beta_1)-2J_1(\beta_1)J_2(\beta_2)J_5(\beta_1)\right]\cos\left(4\omega_1 t+2\omega_2 t+2kt^2\right) \\ &\quad +\left[2J_2(\beta_2)J_3(\beta_1)^2+2J_1(\beta_1)J_2(\beta_2)J_5(\beta_1)\right]\cos\left(6\omega_1 t-2\omega_2 t-2kt^2\right) \\ &\quad +\left[2J_2(\beta_2)J_3(\beta_1)^2+2J_1(\beta_1)J_2(\beta_2)J_5(\beta_1)\right]\cos\left(6\omega_1 t+2\omega_2 t+2kt^2\right) \\ &\quad \left.+2J_2(\beta_2)J_3(\beta_1)J_5(\beta_1)\cos\left(8\omega_1 t-2\omega_2 t-2kt^2\right)\right\} \end{aligned} \tag{3}$$

where η is the responsivity of the PD. Here the fourth-band dual-chirp LFM signals are generated. If the frequency of the RF signal driving MZM1 and the carrier frequency of the LFM signal driving MZM2 meet the condition $\omega_1=2.5\omega_2$, the up-chirp signals with the initial frequency of $2\omega_2$, $7\omega_2$, $12\omega_2$, $17\omega_2$ are spliced with the down-chirp signals with the initial frequency of $3\omega_2$, $8\omega_2$, $13\omega_2$, $18\omega_2$ respectively and the center frequencies of the dual-chirp signals after splicing are $2.5\omega_2$, $7.5\omega_2$, $12.5\omega_2$, $17.5\omega_2$, respectively. The dual-chirp signals have a bandwidth four times of the input chirped signal, which means its TBWP is also quadrupled. From the results of the beat frequency, the amplitude of the up-chirp and the down-chirp in the signal of the same band are different, which is caused by the beat frequencies of the lightwaves of different orders. We can generate optical frequency combs with amplitude differences by reasonably adjusting the

modulation depth of MZM1, so that the amplitude difference between the up- and down-chirp signals in the same band can be minimized. Although the up- and down-chirp signals at lowest and highest center frequency have different amplitudes, it does not affect the measurement accuracy of objects since they are compressed independently in the receiver [27]. Compared with a single-chirp signal, the dual-chirp LFM signal can effectively reduce the range-Doppler coupling and improve the detection resolution in the target scene [28].

## 2. Simulation results

In order to confirm multi-band dual-chirp linearly frequency modulated (LFM) signals generation scheme, the simulation based on Fig.1 was conducted with a laser diode (LD) emitting the lightwave with the central frequency of 193.1 THz, optical power of 10 dBm, and linewidth of 10MHz, respectively, two MZMs with identical half-voltage of 4V and an extinction ratio of 30dB, and a photodiode (PD) with a responsivity of 1 A/W.

The lightwave from the LD is injected into MZM1, biased at the MITP, and is modulated by the RF signal at 10 GHz with voltage amplitude of $V_1$=4.1V, and so a four-tone lightwave is generated with a side-comb suppression ratio (SCSR) of 16.8 dB, as shown in Fig. 2. There is power difference of 2.1dB between the first-order sidebands and the third-order sidebands in order to minimize the amplitude difference between the up-chirp signals and the down-chirp signals after the beating.

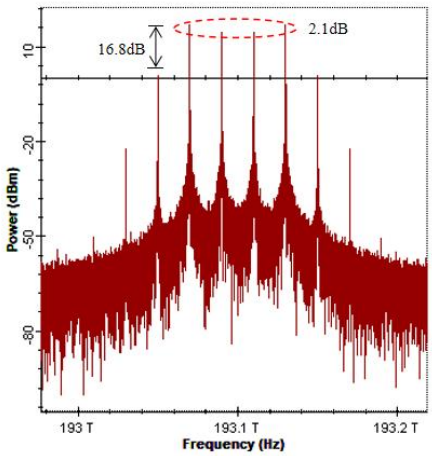


Fig. 2 Optical spectra of the fourth-tone lightwave from MZM1

Then, the four-tone lightwave is injected into MZM2, biased at the MATP to suppress the odd-order sidebands, and is modulated by an up-chirp signal with frequency varying from 4 GHz to 5 GHz and a temporal width of 102.4 ns. As shown in Fig. 3, the lightwave at the center frequency of 193.06THz, 193.08THz, 193.1THz, 193.12THz, 193.14THz clearly have chirp phases and interleaved by the four optical tones, and the chirp phases would be transferred to the generated dual-chirp signals.

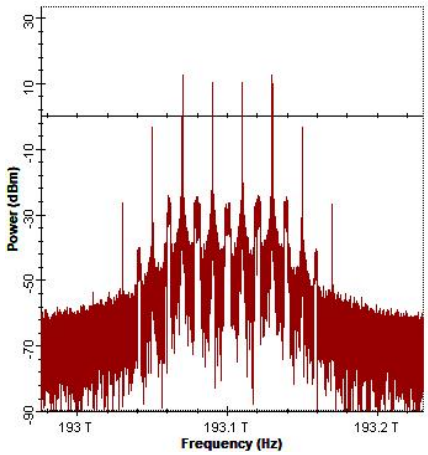


Fig. 3 Optical spectra of the lightwave with chirped phase from MZM2

The lightwave with chirped phases is detected by a square-law photodiode pair, the output photocurrent includes four dual-chirp LFM signals with center frequencies of 10 GHz, 30 GHz, 50 GHz, and 70 GHz. Fig.4(a) and (b) shows the waveform and electrical spectrum including the four-band dual-chirp signals within a duration of 102.4 ns, respectively. The spectrum in Fig.4(b) shows that each of the four-band dual-chirp LFM signals have a bandwidth of 4GHz. Some interferences can be found near 20GHz, 40GHz and 60GHz frequencies. Since these interferences are not overlapped with the desired LFM signal, they can be eliminated by filtering. According to the spectra, the RF spurious suppression ratio (RFSSR) can reach 23.2 dB, which is limited by the higher-order sidebands still exist although their amplitudes are small, as shown in Fig. 2. Fig. 4(c) shows the time-frequency diagram of the waveform extracted by short-time Fourier transform (STFT). It can be seen that each of the four-band LFM signals with center frequencies of 10GHz, 30GHz, 40GHz and 70GHz have both positive and negative chirps.

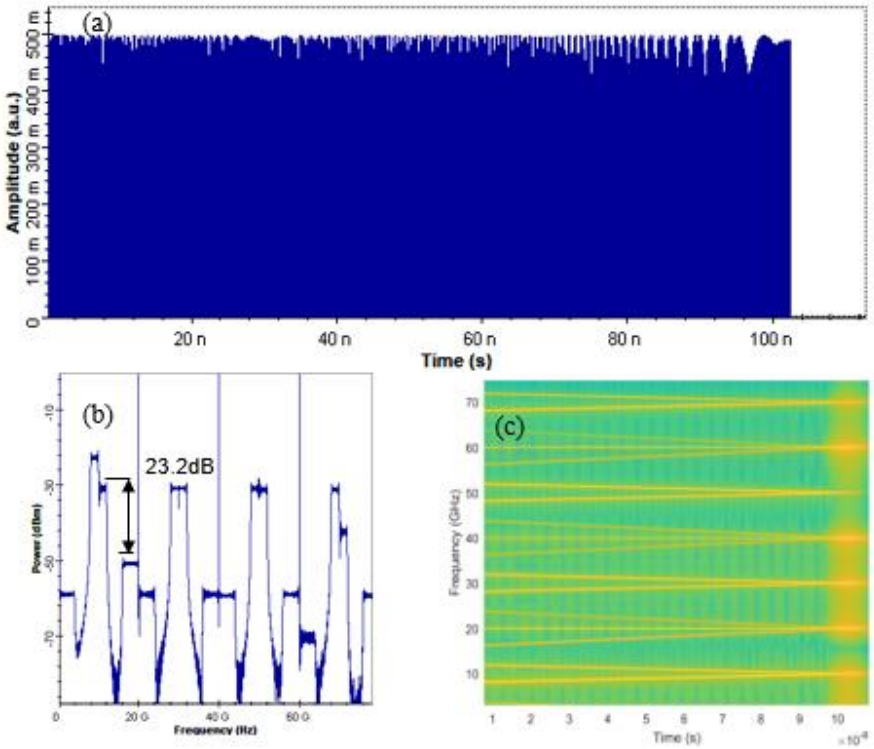


Fig.4 The electrical spectra (a), domain waveform (b) and instantaneous frequency-time diagram (c) of the generated multi -band dual-chirp microwave waveform.

In order to further check the performance of the generated dual-chirp LFM signals, the electric bandpass filters are utilized to select the dual-chirp signals at the center frequency of 10GHz, 30GHz, 50GHz and 70GHz. For each band of the generated dual-chirp microwave waveform, it has a carrier frequency of 10 GHz, a bandwidth of 4 GHz, and a duration of 102.4 ns. The bandwidths of the generated dual-chirp signal is four times that of the driving chirp signal, and TBWP is about 409.6. The autocorrelation function of the generated dual-chirp signal at 10 GHz band is calculated based on the simulation results, as shown in Fig. 5, it can be seen that it has a peak side lobe rate (PSLR) of about 15.31 dB, the full-width at half maximum (FWHM) is 0.22ns, and the PCR is 465.5 approximately. It can be seen that PCR is approximately equal to TBWP. This means that the generated dual-chirp LFM signal has good autocorrelation performance. The dual-chirp waveforms at the center frequency of 30 GHz, 50 GHz and 70 GHz also have a similar performance as that of the 10GHz.

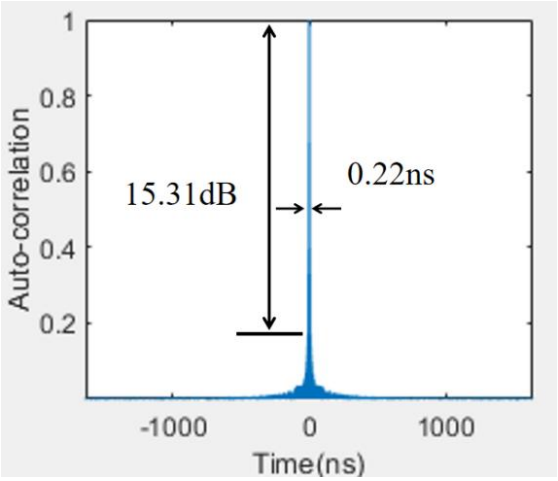


Fig.5 The autocorrelation function of the generated four-band dual-chirp signals at carrier frequency of 10 GHz.

To verify the detection advantage of the obtained signal, ambiguity functions are investigated. Fig.6(a) shows the ambiguity function of the 102.4ns time duration, 4GHz bandwidth and central frequency at 10 GHz dual-chirp LFM signal. The ambiguity function has a peak located at origin, while the sidelobes are effectively decreased. Thus, the range-Doppler coupling is suppressed and the range-Doppler resolution is effectively improved. Fig. 6(b) shows the −3 dB contour maps of the ambiguity functions or the generated dual-chirp signals at 10 GHz, and the ambiguity function has a large −3 dB contour map. Therefore, the dual-chirp LFM signal has good range-Doppler resolution.

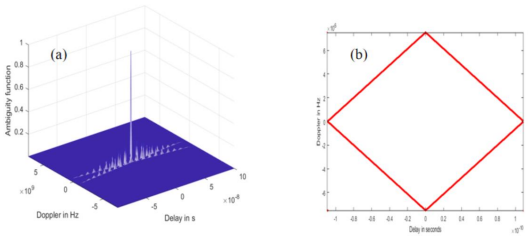


Fig.6 (a) The ambiguity function and (b) -3dB contour maps of the ambiguity functions with the generated signals at 10 GHz.

## 3. Conclusion

In this paper, we propose a scheme to generate multi-band dual-chirp linearly frequency modulated (LFM) signals with quadruple chirp bandwidth, which has been verified by simulation. The proposed scheme can expand the low-frequency single-chirp signal into a four-band dual-chirp

LFM signal with a higher center frequency and the quadruple bandwidth. The ambiguity function and autocorrelation performance are analyzed, and the results show good performance. The proposed scheme provides a simple and effective way to generate multi-band dual-chirp LFM signal with a large time-bandwidth product (TBWP), which is expected to be widely used in modern radar.

In this study, we present a novel scheme for generating multi-band dual-chirp linearly frequency modulated (LFM) signals with quadruple chirp bandwidth. The effectiveness of the proposed scheme has been validated through extensive simulations. Our scheme offers a straightforward and efficient approach to expand a low-frequency single-chirp signal into a four-band dual-chirp LFM signal with an increased center frequency and quadruple bandwidth. To assess the performance of the generated signals, we analyze the ambiguity function and autocorrelation characteristics. The results demonstrate excellent performance in both aspects. Overall, our proposed scheme provides a practical and efficient solution for generating multi-band dual-chirp LFM signals with a significantly larger time-bandwidth product (TBWP). This advancement holds great promise for widespread adoption in modern radar systems.

## Acknowledgments

This work was supported in part by the National Natural Science Foundation of China (6169019 5) and the Fund of State Key Laboratory of IPOC (IPOC2020ZT06).

## Disclosures

The authors declare no conflicts of interest.

## Reference

[1] S. L. Pan, D. Zhu, and F. Z. Zhang, “Microwave photonics for modern radar system, Trans. Nanjing Univ. Aeronaut. Astronaut.”, Vol. 31, no. 3, pp.219-240,2014.

[2] D.K. Barton, Radar System Analysis and Modeling, Artech House, Norwood,MA, USA, 2005.

[3] A. Rashidinejad, Y . Li, and A. M. Weiner, “Recent advances in programmable photonic-assisted ultrabroadband radio-frequency arbitrary waveform generation,” IEEE J. Quantum Electron., vol. 52, no. 1, Jan. 2016, Art. no. 0600117.

[4] J. Ye, L.S. Yan, H.J. Wang, et al., Photonic generation of microwave frequency shift keying signal using a polarization maintaining FBG, IEEE Photon. J. 10 (3) (2017) 5501108.

[5] J.D. McKinney, D. E. Leaird, A.M. Weiner, “Millimeter-wave arbitrary waveform generation with a direct space-to time pulse shaper,” Opt. Lett. 27 (15) (2002) 1345-1347.

[6] Y. L. Liu, J. Liang, “Theoretical investigation of photonic generation of frequency quadrupling linearly chirped waveform with large tunable range,” Opt. Express, vol. 25, no. 14, pp.16196-16203, Jul.2017.

[7] W. Li, W. Wang, W. Sun, et al., “Photonic generation of arbitrarily phase-modulated microwave signals based on a single DDMZM,” Opt. Express 22 (7)(2014) 7446–7457.

[8] C. Wang, J.P. Yao, “Photonic generation of chirped millimeter-wave pulses based on nonlinear frequency-to-time mapping in a nonlinearly chirped fiber Bragg grating,” IEEE Trans. Microw. Theory Tech. 56 (2) (2008) 542–553.

[9] Y. L. Liu, J. Liang, “Theoretical investigation of photonic generation of frequency quadrupling linearly chirped waveform with large tunable range,” Opt. Express, vol. 25, no. 14, pp.16196-16203, Jul.2017.

[10] Y. Zhang, X. Ye, S. Pan, “Photonic generation of linear frequency-modulated waveform with improved time-bandwidth product,” in: Proc. IEEE 2015 Int. Top. Meet. Microw. Photon. Paper WeB.6, 2015.

[11] X. C. Wang, J. X. Ma, “Generation of frequency septupled chirped microwave waveforms with increased TBWP based on two cascaded polarization modulators,” Opt. Comms, 424 (2018) 1–6.

[12] Y. X. Xu, T. Jin, “Photonic generation of dual-chirp waveforms with improved Time-Bandwidth Product,” IEEE Photon. Technol. Lett., vol. 29, no. 15, pp.1253-1256, Aug, 2017.

[13] D. Zhu “Dual-Chirp microwave waveform generation using a dual-parallel Mach–Zehnder modulator,” IEEE Photon. Technol. Lett., vol. 27, no. 13, pp.1410-1413, Jul. 2015.

[14] D. Zhu, W. Xu, Z. Wei, “Multi-frequency phase-coded microwave signal generation based on polarization modulation and balanced detection”, Opt. Lett. 41 (1) (2017) 107–110.

[15] P. Ghelfi, F. Laghezza, F. Scotti, et al., “Photonics for radars operating on multiple coherent bands”, J. Lightwave Technol. 34 (2) (2016) 500–507.

[16] Y. Chen, J. Yao, “Simultaneous multi-frequency phase-coded microwave signal generation at six different frequencies using a DP-BPSK modulator”, J. Lightw. Technol. 37 (10) (2019) 2293–2299.

[17] K. Zhang, S. H. Zhao, “Photonic generation of multi-frequency dual-chirp microwave waveform with multiplying bandwidth,” Results in Physics.,13(2019)10226.

[18] K. Zhang, S. H. Zhao, “Photonic generation of multi-frequency dual-chirp microwave waveform with multiplying bandwidth,” Results in Physics.,13(2019)10226.

[19] Y. X. Xu, T. Jin, “Photonic generation of dual-chirp waveforms with improved Time-Bandwidth Product,” IEEE Photon. Technol. Lett., vol. 29, no. 15, pp.1253-1256, Aug, 2017.

[20] X. Li, S. Zhao, Z. Zhu, et al., “Photonic generation of frequency and bandwidth multiplying dual-chirp microwave waveform”, IEEE Photonics J. 9 (3) (2017) 1–14.

[21] W. Chen, D. Zhu, C. Xie, et al., “Photonics-based reconfigurable multi-band linearly frequency-modulated signal generation”, Opt. Express 26 (25) (2018)32491–32499.

[22] Haowen Zhang, Jianxin Ma & Junyi Zhang (2021) Flexible Multi-band Dual-chirped Microwave Waveforms Generation with Double Bandwidth, Fiber and Integrated Optics, 40:4-6, 276-291, DOI: 10.1080/01468030.2021.2014606

[23] Zhang K, Xuan Li, et al. “Photonic-based dual-chirp microwave waveforms generation with multi-carrier frequency and large time-bandwidth product”. Opt Commun 2020;474:126076.

[24] K. W. Holman, “200-GHz 8-μs LFM optical waveform generation for high-resolution coherent imaging,” in Proc. 19th Coherent Laser Radar Conf., 2018, Art, no. Th7.

[25] Y. Xu, T. Jin, H. Chi, S. Zheng, X. Jin and X. Zhang, “Photonic Generation of Dual-Chirp Waveforms With Improved Time-Bandwidth Product,” IEEE Photon. Technol. Lett., vol. 29, no. 15, pp. 1253-1256, 1 Aug.1, 2017.

[26] A. A. Dotan and I. Rusnak, “Method of measuring closing velocity by transmitting a dual-chirp signal,” in Proc. 26th IEEE Conf. Elect. Electron. Eng. Israel, Eilat, Israel, Nov. 2010, pp. 000258–000262.

[27] J. X. Zhang, W. J. Jiang, Y. Yu, “Photonics-based simultaneous measurement of distance and velocity using multi-band LFM microwave signals with opposite chirps,” Opt. Express 27(20), 27580-27591 (2019).